RSC Advances

ROYAL SOCIETY OF CHEMISTRY

www.rsc.org/advances

Ultrasensitive electrochemical assay of hydrogen peroxide and glucose based on PtNi alloy decorated MWCNTs

He Mei, Huimin Wu*, Wenqin Wu, Shengfu Wang, Qinghua Xia

Hubei Collaborative Innovation Center for Organic Chemical Materials & Key Laboratory for the Synthesis and Application of Organic Functional Molecules, Ministry of Education & College of Chemistry & Chemical Engineering, Hubei University, Wuhan 430062, PR China

* Corresponding author. Tel.: 86 18971479006; Fax: 86 27 88663043

E-mail address: whm267@126.com

Abstract: A novel electrochemical assay based on PtNi/MWCNTs nanocomposites was designed for ultrasensitive detection of hydrogen peroxide and glucose. The PtNi/MWCNTs nanocomposites have been synthesized by chemical reduction method and were investigated by X-ray diffraction, transmission electron microscopy, and electrochemical testing. The results demonstrated that the PtNi/MWCNTs nanocomposites exhibited excellent electrocatalytic activity toward hydrogen peroxide and glucose. The electrocatalytic reduction of hydrogen peroxide showed a wide linear range from 0.2 μM to 24.6 mM, with a high sensitivity of 2123.1 μA mM^{-1} cm^{-2} and a detection limit of 60 nM (S/N =3). At the same time, amperometric sensing of glucose was realized in a linear range from 0.1 μM to 9.0 mM, with a excellent sensitivity of 85910.0 μA mM^{-1} cm^{-2}. The present hybrid system also exhibited a good performance in terms of long-time stability, reproducibility and anti-interference ability.

Keywords: PtNi alloy; MWCNTs; hydrogen peroxide; glucose; non-enzymatic sensor

1 Introduction

Due to its unique electronic, optical, and catalytic properties,[1-3] metal nanoparticles, especially platinum (Pt) nanoparticles are widely used in construction of nonenzymatic hydrogen peroxide or glucose sensors.[4-9] But it also possess some drawbacks, such as slow kinetics, low sensitivity and poor selectivity.[10-12] Modifying Pt surfaces with ad-metals to form bimetallic alloy can significantly alter its surface catalytic reactivity.[13-16] Among various Pt-based bimetallic alloys, PtNi alloy has been

widely investigated in the field of fuel cell [17,18] and shows superior electrocatalytic activity for carbon monoxide [19] and methanol [20] oxidation. This might be attributed to the observations that nickel (Ni), as one of the 3d metals, shows a dramat ically synergistic effect to enhance the electrochemical activity of Pt. [21-23]

Carbon nanomaterial such as carbon nanotubes (CNTs) and graphene [24] show unique electronic structures, chemically active surface, high electrical conductivity, high chemical stability, and good bio-compatibility,[25-27] so are widely used in the fields of dye-sensitized solar cells,[28, 29] supercapacitors,[30, 31] biosensors,[32, 33] especially electrochemical sensors.[34] In recent reports, CNTs has been utilized to enhance the electrocatalytic activity of alloy. It can avoid the alloy precipitate or aggregate, resulting to accelerate the electron transfer and enhance the sensitivity of the sensors.

In this paper, we report a novel nonenzymatic electrochemical hydrogen peroxide and glucose sensor based on PtNi/MWCNTs. It showed high electrocatalytic activity toward hydrogen peroxide and glucose.

2 Material and methods

2.1 Chemicals and reagents

Chloroplatinic acid hexahydrate ($H_2PtCl_6 \cdot 6H_2O$), nickel chloride hexahydrate ($NiCl_2 \cdot 6H_2O$), multi-walled carbon nanotubes (MWCNTs) were purchased from Aldrich. The pristine carbon black sample was purchased from Cabot Australasia Pty. Ltd., Australia (XC-72). Sodium chloride (NaCl), sodium borohydride ($NaBH_4$), hydrogen peroxide (H_2O_2), glucose, sulphuric acid and nitric acid were purchased from Sinopharm Chemical Reagent Co.,Ltd. Ascorbic acid (AA), fructose, uric acid

(UA), chitosan and acetamidophenol (AAP) were purchased from Aladdin. Human blood serum samples was obtained from ZiJing hospitial (Wuhan city, Hubei province) without any other pretreatment before using. All experiments were performed in compliance with the relevant laws and institutional guidelines. A 0.1 M phosphate buffer solution (PBS, 0.1 mol L^{-1}, pH 7.0) containing 0.15 M NaCl was prepared using $Na_2HPO_4 \cdot 12H_2O$ and KH_2PO_4. All aqueous solutions were prepared with analytical grade chemicals and deionized water.

2.2 Synthesis of PtNi/C nanocomposites

Before using, the MWCNTs were acid-treated by stirring in the mixed acid solution, H_2SO_4:HNO_3 (volume ratio)=1:3 for 7 hours to introduce carboxylic acid groups according to the literature,[35] then the MWNTs were washed with deionized water to neutralization, and dried at 80 °C, overnight.

Synthesis of PtNi/C nanocomposites was similar to our previous reports.[36, 37] Briefly, $NiCl_2 \cdot 6H_2O$ (18.7 mg) and $H_2PtCl_6 \cdot 6H_2O$ (40.8 mg) was dissolved in 40 mL of acid-treated MWCNTs or XC-72 suspension (2 mg/mL, suspended in deionized water) under vigorous stirring for about 0.5 h. After that the mixed solution was slowly heated to 138°C under nitrogen atmosphere, and 10 mL of freshly prepared $NaBH_4$ solution was added dropwise. The black suspension then cooled down to room temperature and washed 3-4 times with ethanol. Finally, the powder was dried at 60°C in a vacuum oven overnight.

2.3 Preparation of the modified glassy carbon electrode (GCE)

Before modification, the GCE (geometric area=7.1 mm^2) was polished to mirror

smoothness with 0.05 μm alumina powder, then rinsed with deionized water and ethanol in an ultrasonic bath, and dried in air. Catalyst ink was prepared by mixing 3.0 mg of the prepared PtNi/C nanocomposites with 0.5 mL chitosan (0.5%) and sonicated for 1 h to obtain well dispersed suspension. 20 μL catalyst ink was dropped onto the GCE and dried before electrochemical experiments.

2.4 Apparatus and electrochemical measurements

X-ray diffraction patterns were obtained with a GBC MMA X-ray diffractometer with Cu Kα radiation. Transmission electron microscopy (TEM) was performed using a JEOL JEM 2011 TEM facility. The morphologies and distributions were investigated by field emission gun scanning electron microscopy (FEG-SEM) using a JEOL 7001F instrument. Electrochemical measurements were performed with a CHI 660E electrochemical workstation (CH Instrument Company, Shanghai, China). A conventional three-electrode system cell was employed. The modified GCE was used as the working electrode. The counter electrode was Pt foil, and the reference electrode was a saturated calomel electrode (SCE). So all potentials are reported with respect to the SCE throughout this paper.

3 Results and discussion

3.1 Characterization of the PtNi/C

Fig.1 shows the TEM of the acid-treated MWCNTs (A) and PtNi/MWCNTs (B). It was found that PtNi alloy nanoparticles are deposited on the surface of MWCNTs without obvious aggregation. Fig.1 (C) shows the FEG-SEM of a typical

PtNi/MWCNTs nanocomposites. Compared with PtNi/XC-72 nanocomposites (Fig.1 (D)), it can be seen there are many open porous structure with irregular pore in the PtNi/MWCNTs nanocomposites. This may supply more surface-active sites for the adsorption of analyte and enhance the electrocatalytic activity of the PtNi nanoparticles. Fig.1 (E) displays the XRD patterns of PtNi/MWCNTs (a), PtNi/XC-72 (b) and Pt/XC-72 (c) nanocomposites. The first sharp and high intensity diffraction peak (curve a) at about 25.9^{o} can attribute to (002) hexagonal graphite structure, while the broad and low intensity diffraction peaks (curve b and c) at about 24.3^{o} represent amorphous carbon. The diffraction peaks of PtNi/MWCNTs and PtNi/XC-72 at about 40.3^{o}, 46.9^{o}, corresponding to the reflection planes (111) and (200) of the face-centered cubic Pt crystals,[38] respectively. Compared with Pt/XC-72, the major diffraction peaks of PtNi/C catalysts are gradually shifted to higher 2θ angles (39.7^{o}, 46.0^{o}), indicating an alloy formation between Pt and Ni.[39] The absence of any diffraction peaks of Ni and its oxides structures also suggests that Ni atoms had entered into the crystal lattice of Pt and formed alloy phase through co-reduction process.[40]

The electrochemical performance of the PtNi/C nanocomposites in nitrogen-saturated 0.5 M H_2SO_4 was shown in Fig.1 (F). The multiple peaks between -0.20 and 0.05 V are attributed to the adsorption/desorption of hydrogen.[41] Such hydrogen adsorption–desorption peaks only appear on the Pt_xM_y alloy catalysts where the Pt percentage is not less than 50% in atomic ratio.[42] As shown in Fig.1 (G), the cyclic voltammograms (CVs) in 5 mM $K_3[Fe(CN)_6]$ with 1 M KCl supporting

electrolyte at different scan rates ranging from 10 mV s^{-1} to 230 mV s^{-1} were used to evaluate the electroactive surface areas of PtNi/MWCNTs, PtNi/XC-72 and GCE electrodes. According to the Randles-Sevcik equation,[43] the actual electroactive surface areas of PtNi/MWCNTs and PtNi/XC-72 electrodes are calculated to be about 0.2681, 0.1581 and 0.0547 cm^2, respectively. The electrochemical active surface area (ECSA) of the PtNi/MWCNTs is 4.9 cm^2/cm^2, which is bigger than that of PtNi/XC-72 (2.9 cm^2/cm^2). This result is believed to be originated from the special structure of MWCNTs and highly dispersed PtNi alloy nanoparticles.[44]

Electrochemical impedance spectroscopy (EIS) was utilized to investigated the electrochemical characteristic of PtNi/C. As shown in Fig.1 (H), the profiles show a semicircular part followed by a linear part. The semicircle diameter equaled to the electron transfer resistance (R_{ct}) at high frequencies. The equivalent circuit used to fit the EIS response was shown in the inset of Fig.1 (H). Where, R_s is the solution resistances, Z_w is Warburg impedance, and C_{dl} is the double layer capacitance. Obviously, the R_{ct} of the PtNi/MWCNTs electrode is smaller than that of PtNi/XC-72. It implied that the MWCNTs was more conductive and could accelerate the electron transfer. This may enhance the sensitivity of the nonenzymatic sensor.

Please, insert Fig.1 here

3.2 Electrocatalytic reduction of hydrogen peroxide on modified electrodes

The electrocatalytic behavior of PtNi/MWCNTs electrode toward different concentrations of hydrogen peroxide was investigated by CVs (Fig.2 (A)). Obviously, the reduction peak current at about -0.4 V increase gradually with increasing concentrations of hydrogen peroxide. Compared with PtNi/XC-72 electrode, the

reduction peak potential on PtNi/MWCNTs electrode shifts positively and the current is higher (Fig.2 (B)). This indicates the higher electrocatalytic activity of PtNi/MWCNTs electrode toward hydrogen peroxide. The improved electrochemical activity of PtNi/MWCNTs is ascribed to the higher ECSA. This well-dispersed functionalized MWCNT can provide a more conductive surface area to separately load PtNi active species on the electrode surface, resulting in a uniform, and active hybrid composite. Thus, this hybrid composite can show specific activity towards hydrogen peroxide.

To investigate the electrocatalytic reduction process on PtNi/MWCNTs electrode, the effect of scan rate on the CVs of PtNi/MWCNTs are shown in Fig.2 (C). The peak currents vary linearly with the square root of scan rates in the range from 5 to 200 mV s^{-1}. It suggests that the electrocatalytic reduction of hydrogen peroxide on PtNi/MWCNTs is a diffusion-controlled process, which is the perfect manner for quantitative determination of hydrogen peroxide.

To enhance the sensitivity and selectivity of the PtNi/MWCNTs electrode for detection of hydrogen peroxide, the selection of a suitable working potential is very important. Fig.2 (D) shows the amperometric response of PtNi/MWCNTs electrode at different potentials. Therefore, -0.45 V is used as the optimum potential for hydrogen peroxide sensing. The results can be explained by that the reduction current of hydrogen peroxide and background current has biggest difference at -0.45 V.

Fig.2 (E) shows amperometric responses of the PtNi/MWCNTs electrode toward different concentration of hydrogen peroxide in 0.1 M PBS at -0.45 V. A good linear relationship was realized between reduction peak current of hydrogen peroxide and its concentration in the range of 0.2 μM - 24.6 mM with a sensitivity of 2123.1 μA mM^{-1}

cm^{-2} and a detection limit of 60 nM (S/N=3).

For practical applications, the selectivity, stability and repeatability of the PtNi/MWCNTs for hydrogen peroxide detection are very important. As shown in Fig.2 (F), well-defined current responses are observed for 0.1 mM hydrogen peroxide, while there are not obvious current response of 0.1 mM UA, 0.1 mM AAP, 0.1 mM AA, and 0.1 mM fructose. It demonstrates that the PtNi/MWCNTs has a good selectivity, which is attributed to the relatively low working potential of -0.45 V used in the determination of hydrogen peroxide. The PtNi/MWCNTs electrode was stored at room temperature for 30 days, the current response to 10 mM hydrogen peroxide can keep 97.9 % of its initial value. Under the same conditions, the current of five-paralleled PtNi/MWCNTs electrodes toward 10 mM hydrogen peroxide were measured with a *RSD* of 2.2%. The results clearly demonstrated the PtNi/MWCNTs possess a good stability and repeatability. According to the Table 1, the PtNi/MWCNTs electrode can be used for practical detection.

Please, insert Fig.2 and Table 1 here

3.3 Electrocatalytic oxidation of glucose on modified electrodes

Fig.3 (A) shows the CVs of PtNi/MWCNTs electrode in 0.1 M PBS (pH7.0) containing different concentrations of glucose. In the absence of glucose, peaks at the range from -0.25 V to -0.6 V and -0.25 V to 0.8 V were assigned to hydrogen desorption and adsorption and the Pt oxide formation/reduction, respectively.[45, 46] When glucose was added into 0.1 M PBS (pH7.0), the oxidative peaks (I, Π) of

glucose were obviously observed and the current increased with increasing glucose concentration. The effects of matrix on electrochemical oxidation of glucose were investigated as shown in Fig.3 (B). The peaks current of the PtNi/MWCNTs are substantially higher than that of the PtNi/XC-72. It suggested that the PtNi/MWCNTs exhibits much better electrocatalytic ability towards glucose than PtNi/XC-72. The well-distributed PtNi NPs on MWCNTs would induce more active sites for the electrocatalytic oxidation of glucose and bring about an efficient electrical network through their direct binding with the MWCNTs. This favorable situation with low transport limitations of substrate would greatly increase the electrocatalytic activity.[47]

The CVs of PtNi/MWCNTs electrode in 0.1 M PBS (pH7.0) containing 6 mM glucose at different scan rates were also investigated (Fig.3 (C)). The peak current of glucose oxidation increases clearly with increasing scan rate in the range of 5-200 mV/s, which demonstrates the electrochemical process is typically surface adsorption-controlled.[46]

Chronoamperometry was utilized to quantitatively detect of glucose at the optimum potential of +0.1 V (Fig.3 (D)). Upon successive additions of glucose into gently stirred 0.1 M PBS (pH 7.0), the oxidation current increased immediately and reached 95% of steady-state value in less than 2 s. The PtNi/MWCNTs electrode gave rise to a excellent sensitivity of 85910.0 μA mM^{-1} cm^{-2} with a linear range from 0.1 μM to 9.0 mM and a detection limit of 30 nM (S/N=3). The huge sensitivity may be related with a high ECSA of the nanocomposites and the synergistic amplification effect of MWCNTs and PtNi nanoparticles.

Biomolecules such as AA, UA, AAP, and fructose commonly exist with glucose, and the concentration of these species is approximately 30 to 50 times less than that of glucose in human blood (4-7 mM). Fig.3 (E) represents the chronoamperometric responses of glucose (0.5 mM) in the presence of 0.5 mM AA, 0.5 mM UA, 0.5 mM AAP, and 0.5 mM fructose in phosphate buffer (pH 7.0). The current responses of these interferences are almost negligible, compared with that of glucose. It indicated that the selectivity of the PtNi/MWCNTs electrode was acceptable. And measurements of five PtNi/MWCNTs electrodes to 6 mM glucose showed similar signals with *RSD* of 0.88%, indicating the satisfactory reproducibility. When the PtNi/MWCNTs electrode was stored at room temperature, the current retained 96.9% of its initial value after 30 days. It indicated that the PtNi/MWCNTs electrode has a good stability.

To verify its workability, the PtNi/MWCNTs electrode was applied to detect the concentration of glucose in human serum samples. Fig.3 (F) shows the amperometric response obtained by injecting 50 μL of 10 mM glucose (a, b, e and f) and 50 μL blood serum (c and d) into 6 mL gently stirred 0.1 M PBS (pH 7.0) at +0.1 V. The concentration of glucose in blood is 85.3 μM, which is consistent with the result obtained from hospital. It indicated that the PtNi/MWCNTs electrode offers an accurate method for determination of glucose in real samples.

We have summarized various hydrogen peroxide and glucose sensors based on Pt-based and Ni-based nanoparticles in Table 2 and Table 3. For hydrogen peroxide sensors, the sensor based on PtNi/MWCNTs shows the excellent sensitivity of

2123.10 μA mM^{-1} cm^{-2}, which is almost 13 times as big as Pt/PPy (164.94 μA mM^{-1} cm^{-2}), [48] and twice as big as NiO/GS (1077.00 μA mM^{-1} cm^{-2}).[49] The detection limit (0.06 μM) is smaller than Pt/PG (0.5 μM) [50] and NP-PdNi (2.1 μM), [23] while is bigger than PtRu/3D GF. [51] And the linear range is the widest in the Table 2. Compared with other glucose sensors listed in Table 3, it is clear that the linear range, detection limit and sensitivity of PtNi/MWCNTs are superior to most of the sensors.

Please, insert Fig.3, Table 2 and Table 3 here

4 Conclusions

In conclusion, the PtNi alloy nanoparticles were successfully synthesized using a co-reduction process with carbon as substrates. The PtNi alloy nanoparticles were well dispersed on acid-treated MWCNTs and showed better electrocatalytic activity toward hydrogen peroxide and glucose than that on XC-72. The PtNi/MWCNTs were used to construct nonenzymatic hydrogen peroxide and glucose sensor, and the resulting sensor can be applied to detect real sample with excellent sensitivity, good stability and reproducibility.

Acknowledgements

We acknowledge financial support from the National Natural Science Foundation of China through a project entitled “The synthesis of Pt-M/C nanoparticles and construction of non-enzymatic electrochemical biosensor” (Grant No. 21205030), and by the Science and Technology Department of Hubei province through a project entitled “The development of electrochemical biosensor based on non-noble metal nanocomposites”(2014CFB548), and by State Key Laboratory of Advanced

Technology for Materials Synthesis and Processing (Wuhan University of Technology，2015-KF-13), and from the Natural Science Fund for Creative Research Groups of Hubei Province of China through a project entitled “Controllable Synthesis and Application of Nano-/microsized Functional Materials”(2014CFA015).

References

1 D. M. Dotzauer, J. H. Dai, L. Sun and M. L. Bruening, *Nano Lett.,* 2006, **6**, 2268.

2 X. S. Fang, L. F. Hu, C. H. Ye and L. D. Zhang, *Pure Appl. Chem.,* 2010, **82**, 2185.

3 N. Gao and X. S. Fang, *Chem. Rev.,* 2015, **115**, 8294.

4 L. Y. Meng, Y. X. Xia, W. G. Liu, L. Zhang, P. Zou and Y. S. Zhang, *Electrochim. Acta,* 2015, **152**, 330.

5 L. T. Hoa, K. G. Sun and S. H. Hur, *Sens. Actuators B,* 2015, **210**, 618.

6 K. Dhara, J. Stanley, T. Ramachandran, G. N. Bipin and T. G. Satheesh Babu, *Sens. Actuators B,* 2014, **195**, 197.

7 Z. D. Xu, L. Z. Yang and C. L. Xu, *Anal. Chem.,* 2015, **87**, 3438.

8 B. He, L. J. Hong, J. Lu, J. G. Hu, Y. Y. Yang, J. H. Yuan and L. Niu, *Electrochim. Acta,* 2013, **91**, 353.

9 X. Y. Ge, Z. X. Li and Q. Yuan, *J. Mater. Sci. Technol.,* 2015, **31**, 645.

10 B. Beden, F. Largeaud, K. B. Kokoh and C. Lamy, *Electrochim. Acta,* 1996, **41**, 701.

11 I. T. Bae, E. Yeager, X. Xing and C.C. Liu, *J. Electroanal. Chem.,* 1991, **309**, 131.

12 C. Chen, Q. J. Xie, D. W. Yang, H. L. Xiao, Y. C. Fu, Y. M. Tan and S. Z. Yao, *RSC Adv.,* 2013, **3**, 4473.

13 S. Ernst and J. J. Heitbaum, *J. Electroanal. Chem.,* 1979, **100**, 173.

14 S. B. Aoun, Z. Dursun, T. Koga, G. S. Bang, T. Sotomura and I. Taniguchi, *J. Electroanal. Chem.,* 2004, **567**, 175.

15 H. F. Cui, J. S. Ye, X. Liu, W. D. Zhang and F. S. Shen, *Nanotechnology*, 2006, **17**, 2334.

16 S. H. Chang, M. H. Yeh, J. Rick, W. N. Su, D. G. Liu, J. F. Lee, C. C. Liu and B. J. Hwang, *Sens. Actuators B,* 2014, **190**, 55.

17 W. M. Daoush and T. Imae, *J. Experiment. Nanosci.,* 2015, **10**, 392.

18 D. J. Guo, S. K. Cui, D. Cheng, P. Zhang, L. Jiang and C. C. Zhang, *J. Power Sources*, 2014, **255**, 157.

19 Y. J. Hu, P. Wu, Y. J. Yin, H. Zhang and C. X. Cai, *Appl. Catal. B: Environ.,* 2012, **111-112**, 208.

20 Y. J. Hu, Q. Shao, P. Wu, H. Zhang and C. X. Ca, *Electrochem. Commun.,* 2012, **18**, 96.

21 M. Mandal, S. Kundu, S. K. Ghosh, T. K. Sau, S. M. Yusuf and T. Pal, *J. Colloid Interf. Sci.,* 2003, **265**, 23.

22 C. X. Xu, A. H. Liu, H. J. Qiu and Y. Q. Liu, *Electrochem. Commun.,* 2011, **13**, 766.

23 D. Y. Zhao and C. X. Xu, *J. Colloid Interf. Sci.,* 2015, **447**, 50.

24 J. H. Zhu, M. J. Chen, Q. L. He, L. Shao, S. Y. Wei and Z. H. Guo, *RSC Adv.,* 2013, **3**, 22790.

25 S. N. Kim, J. F. Rusling and F. Papadimitrakopoulos, *Adv. Mater.,* 2007, **19**, 3214.

26 T. Sainsbury, T. Ikuno, D. Okawa, D. Pacilé, J. M. J. Fréchet and A. Zettl, *J. Phys. Chem. C,* 2007, **111**, 12992.

27 F. H. Li, J. Chai, H. F. Yang, D. X. Han and L. Niu, *Talanta,* 2010, **81**, 1063.

28 S. Quaranta, D. Gozzi, M. Tucci, L. Lazzarini and A. Latini, *J. Power Sources,* 2012, **204**, 249.

29 K. T. Dembele, R. Nechache, L. Nikolova, A. Vomiero, C. Santato, S. Licoccia and F. Rosei, *J. Power Sources,* 2013, **233**, 93.

30 W. Tang, Y. Y. Hou, X. J. Wang, Y. Bai, Y. S. Zhu, H. Sun, Y. B. Yue, Y. P. Wu, K. Zhu and R. Holze, *J. Power Sources,* 2012, **197**, 330.

31 H. Jiang, Y. Dai, Y. Hu, W. Chen and C. Li, *ACS Sustainable Chem. Eng.,* 2014, **2**, 70.

32 L. Liu, Y. Y. Li, L. H. Tian, T. Guo, W. Cao and Q. Wei, *Sens. Actuators B,* 2015, **211**, 170.

33 J. Wang, *Electroanalysis,* 2005, **17**, 7.

34 A. Bathinapatla, S. Kanchi, P. Singh, M. I.Sabela and K. Bisetty, *Biosens. Bioelectron.,* 2015, **67**, 200.

35 A. K. Baytak and M. Aslanoglu, *Sens. Actuators B,* 2015, **220**, 1161.

36 Q. Sheng, H. Mei, H. M. Wu, X. H. Zhang and S. F. Wang, *Sens. Actuators B,* 2014, **203**, 588.

37 H. M. Wu, D. Wexler and G. X. Wang, *J. Alloys Compd.,* 2009, **488**, 195.

38 S. Beyhan, J. M. Léger and F. Kadırgan, *Appl. Catal. B: Environ.,* 2013, **130-131**, 305.

39 G. J. Wang, Y. Z. Gao, Z. B. Wang, C. Y. Du, J. J. Wang and G. P. Yin, *J.Power Sources,* 2010, **195**, 185.

40 I. G. Casella, M. R. Guascito and M. G. Sannazzaro, *J. Electroanal. Chem.,* 1999, **462**, 202.

41 A. Peremans and A. Tadjeddine, *J. Chem. Phys.,* 1995, **103**, 7197.

42 Q.H. Huang, H. Yang, Y.W. Tang, T.H. Lu and D.L. Akins, *Electrochem. Commun.* 2006, **8**, 1220.

43 J. Yang, W. D. Zhang and S. Gunasekaran, *Electrochim. Acta*, 2011, **56**, 5538.

44 Y. J, Hu, P. Wu, H. Zhang and C.X. Cai, *Electrochim. Acta*, 2012, **85**, 314.

45 G. H. Wu, X. H. Song, Y. F. Wu, X. M. Chen, F. Luo and X. Chen, *Talanta,* 2013, **105**, 379.

46 J. P. Wang, D. F. Thomas and A. C. Chen, *Anal. Chem.,* 2008, **80**, 997.

47 H. C. Gao, F. Xiao, C. B. Ching and H. W. Duan, *ACS Appl. Mater. Interfaces,* 2011, **3**, 3049.

48 L. W. Xing, Q. F. Rong and Z. F. Ma, *Sens. Actuators B,* 2015, **221**, 242.

49 W. Liu, H. X. Zhang, B. Yang, Z. J. Li, L. C. Lei and X. W. Zhang, *J. Electroanal. Chem.,* 2015, **749**, 62.

50 J. Liu, X. J. Bo, Z. Zhao and L. P. Guo, *Biosens. Bioelectron.,* 2015, **74**, 71.

51 C. C. Kung, P. Y. Lin, F. J. Buse, Y. H. Xue, X. Yu, L. M. Dai and C. C. Liu, *Biosens. Bioelectron.,* 2014, **52**, 1.

52 H. Kivrak, O. Alal and D. Atbas, *Electrochim. Acta,* 2015, **176**, 497.

53 H. Liu, X. L. Wu, B. Yang, Z. J. Li, L .C. Lei and X. W. Zhang, *Electrochim. Acta,* 2015,**174**, 745.

54 P. Lu, Y. T. Lei, S. J. Lu, Q. Wang and Q. B. Liu, *Anal. Chim. Acta,* 2015, **880**, 42.

55 G. Chang, H. H. Shu, Q. W. Huang, M. Oyama, K. Ji, X. Liu and Y. B. He, *Electrochim. Acta,* 2015, **157**, 149.

56 T. Choi, S. H. Kim, C. W. Lee, H. Kim, S. K. Choi, S. H. Kim, E. Kim, J. Park and H. Kim, *Biosens. Bioelectron.,* 2015, **63**, 325 .

57 P. Lu, Q. B. Liu, Y. Z. Xiong, Q. Wang, Y. T. Lei, S. J. Lu, L. W. Lu and L. Yao, *Electrochim. Acta,* 2015, **168**, 148.

Tables:

Table 1. Amperometric hydrogen peroxide sensor applied to lake water (Shahu, Wuhan city)

Table 2. Comparison of different hydrogen peroxide sensors

Table 3. Comparison of different glucose sensors

Table 1. Amperometric hydrogen peroxide sensor applied to lake water (Shahu, Wuhan city)

Samples	Lake water	Added (μM)	Found (μM)	Recovery (%)
1	Not found	0.25 μM	0.24 μM	96.0%
2	Not found	0.15 mM	0.16 mM	106.7%
3	Not found	1.00 mM	1.01 mM	101.0%

Table 2. Comparison of different hydrogen peroxide sensors

Material	Linear range (mM)	LOD (μM)	Sensitivity ($\mu A\ mM^{-1}\ cm^{-2}$)	Ref.
NP-PdNi	0.05-1.0	2.1	208.60	[23]
PPy/Pt	0.5-6.3	0.6	164.94	[48]
NiO/GS	0.5-4.0	0.4	1077.00	[49]
Pt/PG	0.001-1.447	0.50	341.14	[50]
PtRu/3D GF	0.005-0.02	0.04	1023.10	[51]
Pt-MnO_x	0.002-4	0.7	122.99	[52]
PtNi/MWCNTs	0.0002-24.6	0.06	2123.10	This work

Table 3. Comparison of different glucose sensors

Material	Linear range (mM)	LOD (μM)	Sensitivity ($\mu A\ mM^{-1}\ cm^{-2}$)	Ref.
s-NiO/GD	1.0-10.0	0.9	3613.0	[53]
a-$Ni(OH)_2$	0.00087-10.53	0.08	418.8	[54]
Pt/GOH	5.0-20.0	-	137.4	[5]
PtNCs/graphene	1.0-25.0	30.0	71.9	[55]
CNT-Ni	0.005-2.0	2.0	1384.1	[56]
$Ni(OH)_2$-HS	0.8749-7.781	0.1	223.39	[57]
PtNi/MWCNTs	0.0001-9.0	0.03	85910.0	This work

Figure Captions:

Fig.1 TEM of acid-treated MWCNTs (A) and PtNi/MWCNTs (B) Inset: the corresponding selected area electron diffraction pattern; FEG-SEM image of PtNi/MWCNTs (C) and PtNi/XC-72 (D); (E) X-ray diffraction patterns of PtNi/MWCNTs (a), PtNi/XC-72 (b) and Pt/XC-72 (c); (F) CVs of PtNi/MWCNTs (a), PtNi/XC-72 (b) electrodes in nitrogen-saturated 0.5 M H_2SO_4 electrolyte, Scanning rate: 20 mV s^{-1}; (G) CVs of the PtNi/MWCNTs electrode in 5.0 mM $K_3[Fe(CN)_6]$ solution containing 1.0 M KCl at the different scan rates ranging from 10 mV s^{-1} to 230 mV s^{-1}. Inset : the dependence of the peak current on the square root of the scan rate; (H) EIS of PtNi/MWCNTs (a), PtNi/XC-72 (b) electrodes in 0.5 mM $[Fe(CN)_6]^{3-}/[Fe(CN)_6]^{4-}$ containing 0.5 M KNO_3 solution. Inset: Equivalent circuit mold for impedance plots.

Fig.2 (A) CVs of PtNi/MWCNTs electrode in 0.1 M PBS (pH7.0) containing different concentrations of hydrogen peroxide (0, 5, 10, 20, 30, 40, 50, 60, 70 mM); (B) CVs of PtNi/MWCNTs (a) and PtNi/XC-72 (b) electrode in 0.1 M PBS (pH7.0) containing 10 mM hydrogen peroxide, Scanning rate: 20 mV s^{-1}; (C) CVs of PtNi/MWCNTs electrode in 0.1 M PBS (pH7.0) in the presence of 10 mM hydrogen peroxide at various scan rates: 5,10, 20, 40, 60, 80, 100, 120, 140, 160, 180, 200 mV s^{-1}. (D) Amperometric response of PtNi/MWCNTs electrode at different potentials from -0.35 V to -0.55 V with successive additions of 0.1 mM hydrogen peroxide into 0.1 M PBS (pH7.0); (E)

Amperometric response of PtNi/MWCNTs electrode with successive additions of hydrogen peroxide into stirring 0.1 M PBS (pH7.0) at -0.45 V. (Inset: amperometric current responses vs hydrogen peroxide concentration); (F) Amperometric response of the PtNi/MWCNTs electrode at -0.45 V for the sequential addition of 0.1 mM hydrogen peroxide, 0.1 mM UA, 0.1 mM AAP, and 0.1 mM AA, and 0.1 mM fructose into 0.1 M PBS (pH7.0).

Fig.3 (A) CVs of PtNi/MWCNTs electrode in 0.1 M PBS (pH7.0) containing different concentrations of glucose (0, 2, 6, 8 mM) at the scan rate of 20 mV s^{-1} ; (B) CVs of PtNi/MWCNTs (a) and PtNi/XC-72 (b) electrodes in 0.1 M PBS (pH7.0) containing 6 mM glucose at the scan rate of 20 mV s^{-1} ; (C) CVs of PtNi/MWCNTs electrode in 0.1 M PBS (pH7.0) in the presence of 6 mM glucose at various scan rates: 5,10, 20, 40, 60, 80, 100, 120, 140, 160, 180, 200 mV s^{-1}. (D) Amperometric response of PtNi/MWCNTs electrode with successive addition of glucose into stirring 0.1 M PBS (pH7.0); (E) Amperometric response of the PtNi/MWCNTs electrode at +0.1 V for the sequential addition of 0.5 mM AA, 0.5 mM UA, 0.5 mM AAP, 0.5 mM fructose and 0.5 mM glucose into 0.1 M PBS (pH7.0); (F) Amperometric response of PtNi/MWCNTs electrode to glucose and serum samples tested in 0.1 M PBS (pH7.0) at +0.1 V. (a, b, e, f are for 83.3 μM glucose solutions and c, d are blood serum).

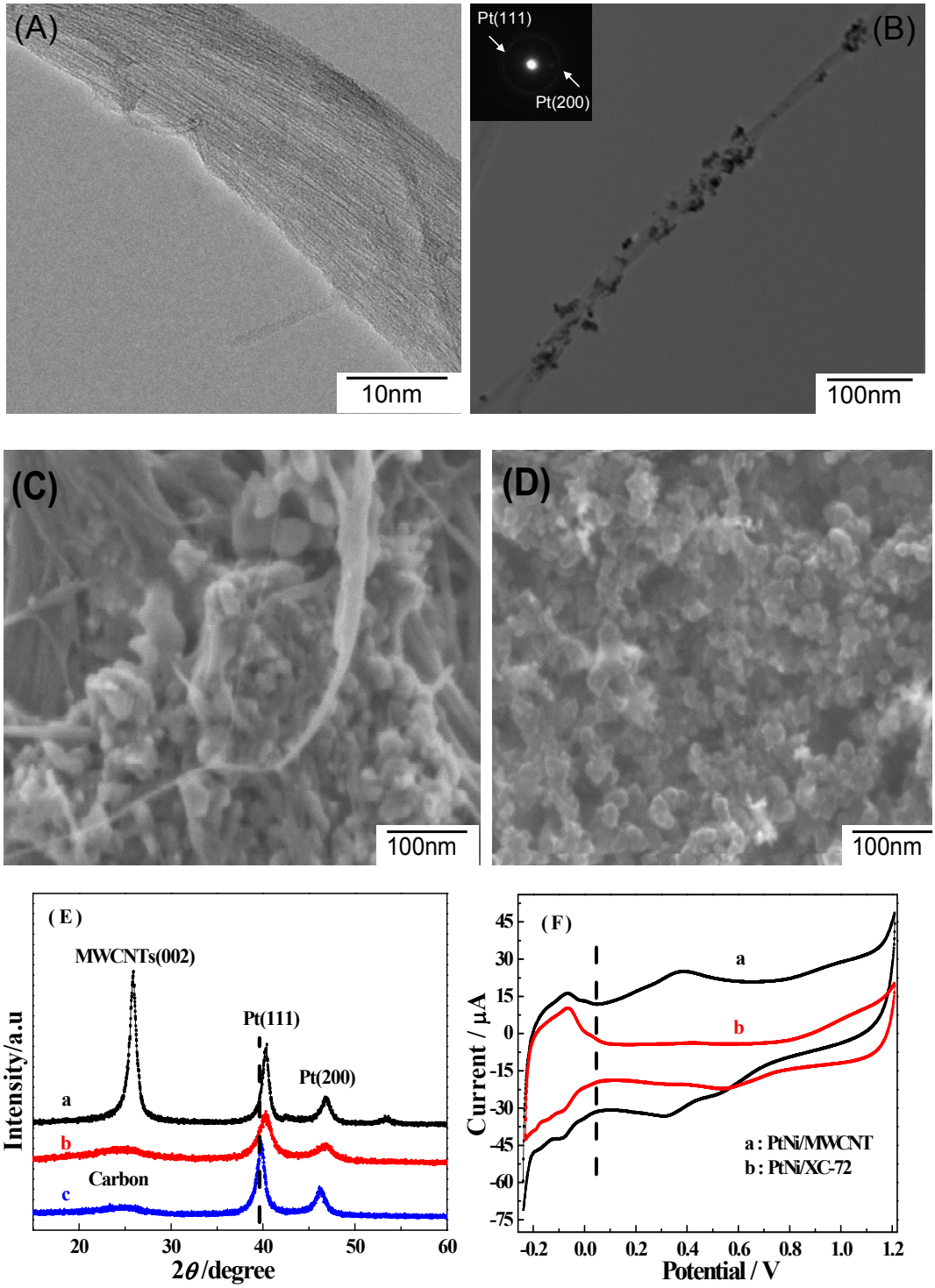

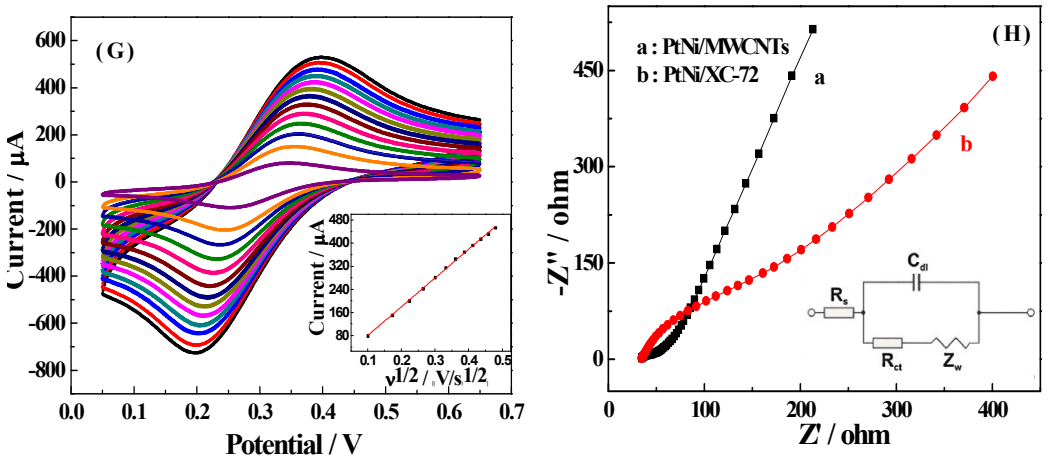

Fig.1 TEM of acid-treated MWCNTs (A) and PtNi/MWCNTs (B). Inset: the corresponding selected area electron diffraction pattern; FEG-SEM image of PtNi/MWCNTs (C) and PtNi/XC-72 (D); (E) X-ray diffraction patterns of PtNi/MWCNTs (a), PtNi/XC-72 (b) and Pt/XC-72 (c); (F) CVs of PtNi/MWCNTs (a), PtNi/XC-72 (b) electrodes in nitrogen-saturated 0.5 M H_2SO_4 electrolyte, Scanning rate: 20 mV s^{-1}; (G) CVs of the PtNi/MWCNTs electrode in 5.0 mM $K_3[Fe(CN)_6]$ solution containing 1.0 M KCl at the different scan rates ranging from 10 mV s^{-1} to 230 mV s^{-1}. Inset : the dependence of the peak current on the square root of the scan rate; (H) EIS of PtNi/MWCNTs (a), PtNi/XC-72 (b) electrodes in 0.5 mM $[Fe(CN)_6]^{3-}$/$[Fe(CN)_6]^{4-}$ containing 0.5 M KNO_3 solution. Inset: Equivalent circuit mold for impedance plots.

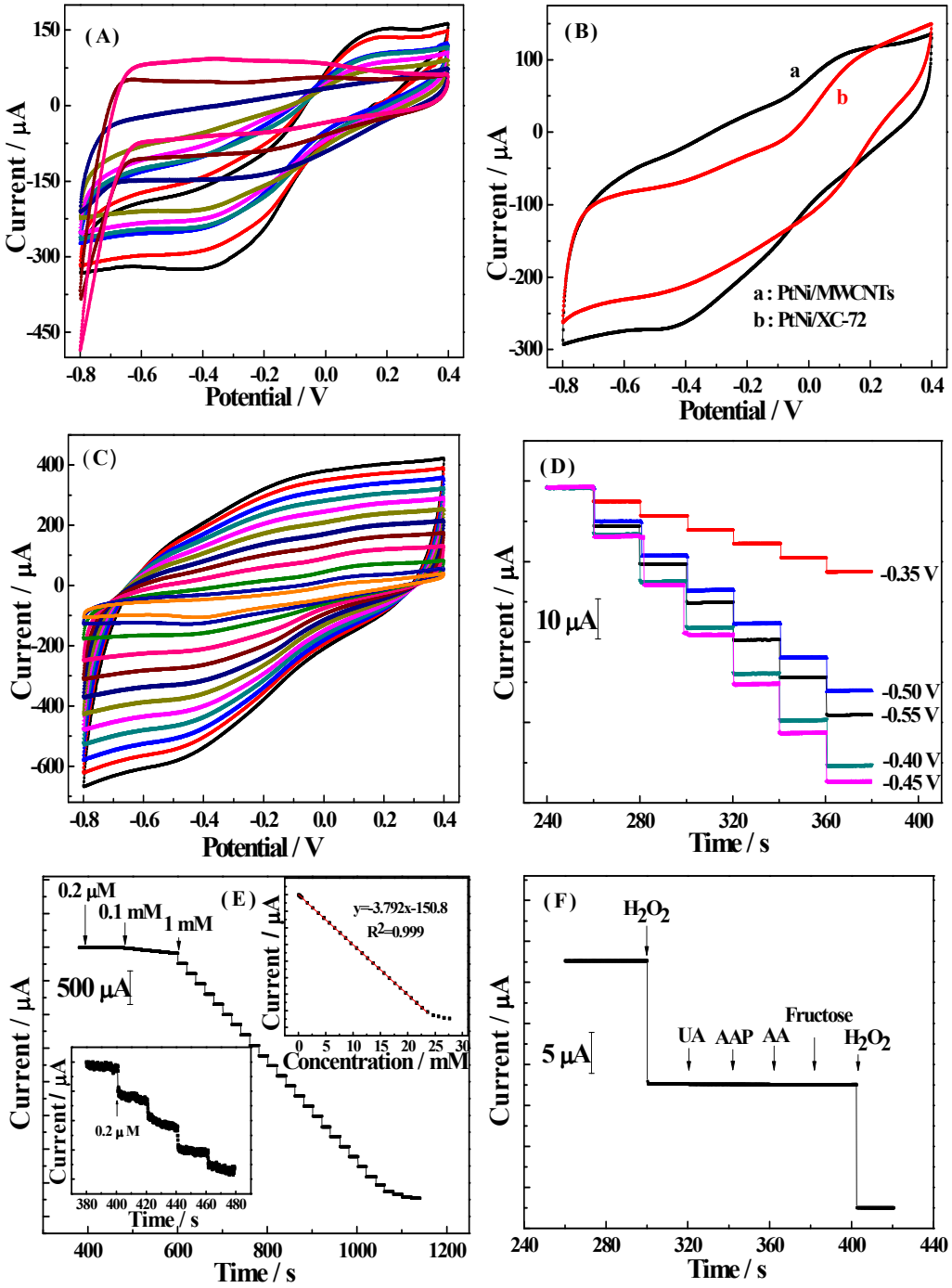

Fig.2 (A) CVs of PtNi/MWCNTs electrode in 0.1 M PBS (pH 7.0) containing different concentrations of hydrogen peroxide (0, 5, 10, 20, 30, 40, 50, 60, 70 mM); (B) CVs of PtNi/MWCNTs (a) and PtNi/XC-72 (b) electrode in 0.1 M PBS (pH7.0) containing 10 mM hydrogen peroxide, Scanning rate: 20 mV s^{-1}; (C) CVs of PtNi/MWCNTs electrode in 0.1 M PBS (pH7.0) in the presence of 10 mM hydrogen peroxide at various scan rates: 5,10, 20, 40, 60, 80, 100, 120, 140, 160, 180, 200 mV

s^{-1}. (D) Amperometric response of PtNi/MWCNTs electrode at different potentials from -0.35 V to -0.55 V with successive additions of 0.1 mM hydrogen peroxide into 0.1 M PBS (pH7.0); (E) Amperometric response of PtNi/MWCNTs electrode with successive additions of hydrogen peroxide into stirring 0.1 M PBS (pH7.0) at -0.45 V. (Inset: amperometric current responses vs hydrogen peroxide concentration); (F) Amperometric response of the PtNi/MWCNTs electrode at -0.45 V for the sequential addition of 0.1 mM hydrogen peroxide, 0.1 mM UA, 0.1 mM AAP, and 0.1 mM AA, and 0.1 mM fructose into 0.1 M PBS (pH7.0).

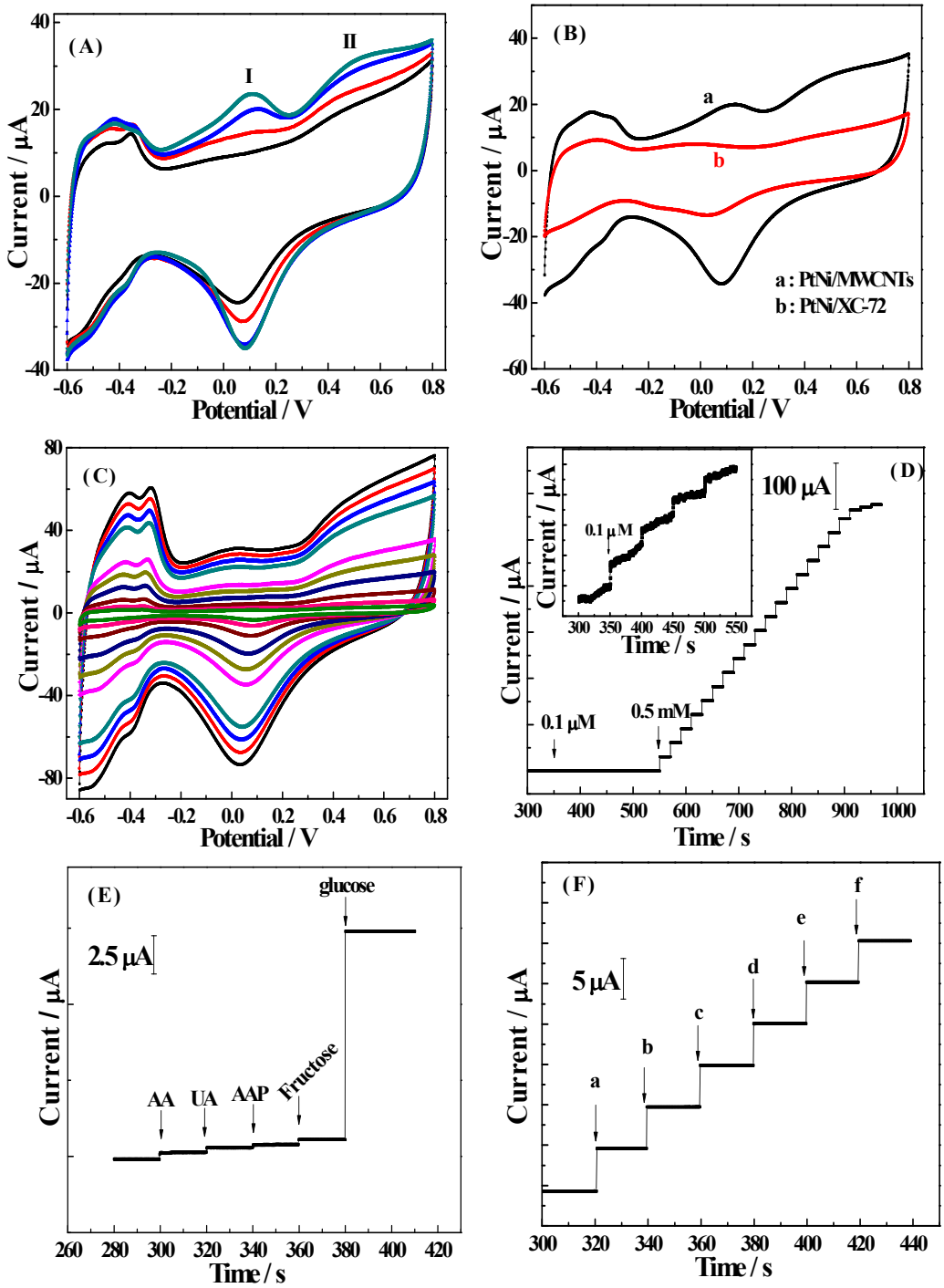

Fig.3 (A) CVs of PtNi/MWCNTs electrode in 0.1 M PBS (pH7.0) containing different concentrations of glucose (0, 2, 6, 8 mM) at the scan rate of 20 mV s^{-1} ; (B) CVs of PtNi/MWCNTs (a) and PtNi/XC-72 (b) electrodes in 0.1 M PBS (pH 7.0) containing 6 mM glucose at the scan rate of 20 mV s^{-1} ; (C) CVs of PtNi/MWCNTs electrode in

0.1 M PBS (pH 7.0) in the presence of 6 mM glucose at various scan rates: 5,10, 20, 40, 60, 80, 100, 120, 140, 160, 180, 200 mV s^{-1}. (D) Amperometric response of PtNi/MWCNTs electrode with successive addition of glucose into stirring 0.1 M PBS (pH7.0); (E) Amperometric response of the PtNi/MWCNTs electrode at +0.1 V for the sequential addition of 0.5 mM AA, 0.5 mM UA, and 0.5 mM AAP, 0.5 mM fructose and 0.5 mM glucose into 0.1 M PBS (pH7.0); (F) Amperometric response of PtNi/MWCNTs electrode to glucose and serum samples tested in 0.1 M PBS (pH7.0) at +0.1 V. (a, b, e, f are for 83.3 μM glucose solutions and c, d are blood serum).

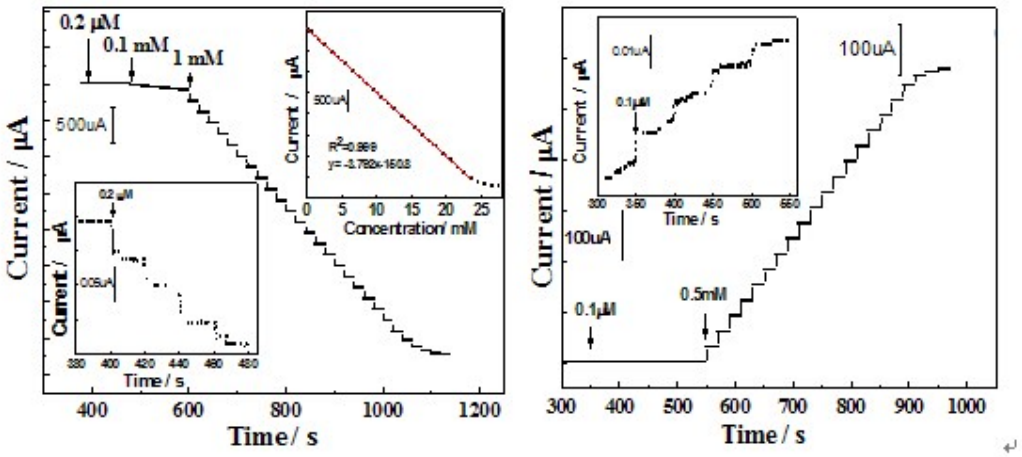

A electrochemical sensor based on PtNi/MWCNTs can detect hydrogen peroxide and glucose with wide linear range and high sensitivity.